Advances in Geo-Energy Research

Vol. 14, No. 1, p. 25-33, 2024

Original article

From traditional extrapolation to neural networks: Time-depth relationship innovations in the subsurface characterization of Drava Basin, Pannonian Super Basin

Ana Kamenski[1], Marko Cvetković[2]*, Josipa Kapuralić[2], Iva Kolenković Močilac[2], Ana Brcković[2]

[1]*Department of Geology, Croatian Geological Survey, Zagreb 10000, Croatia*

[2]*Faculty of Mining, Geology and Petroleum Engineering, University of Zagreb, Zagreb 10000, Croatia*

Keywords:
Well logs
time-to-depth relationship
seismic interpretation
artificial neural networks
Pannonian Super Basin

Cited as:
Kamenski, A., Cvetković, M., Kapuralić, J., Kolenković Močilac, I., Brcković, A. From traditional extrapolation to neural networks: Time-depth relationship innovations in the subsurface characterization of Drava Basin, Pannonian Super Basin. Advances in Geo-Energy Research, 2024, 14(1): 25-33. https://doi.org/10.46690/ager.2024.10.05

Abstract:
The estimation of time-to-depth relationships can prove challenging in regions with rare acoustic logs. This study focuses on the eastern part of the Drava Basin in north Croatia, chosen as a mature hydrocarbon exploration area with abundant geophysical and well data. As only a small portion of wells have well log measurements or seismic profiling performed, a time-to-depth extrapolation is often performed, which potentially results in the erroneous placement of well log markers in the time domain and affects the interpretation of seismic sections or volumes. This study proposes a novel methodology for predicting two-way travel time values in wells without vertical seismic profiling or acoustic logging. This research evaluates the parameters for the characterization of the velocity distribution in the subsurface and the efficiency of artificial neural networks versus conventional methods for this task. The constructed artificial neural network model has a correlation coefficient above 0.99 for the training, testing, and validation datasets, with a mean absolute error of approximately 25 milliseconds for each network. Artificial neural networks proved to have a lesser error in predicting the two-way time and are not sensitive to outlier values.

1. Introduction

The subsurface of the Drava Basin in North Croatia proved to be a rich hydrocarbon exploration area at a Pannonian Super Basin scale (Velić et al., 2012a, 2012b). This has led to extensive exploration activities in the last 70 years, resulting in a substantial amount of geophysical and geological data. The data collected outside the active hydrocarbon exploitation blocks is available for research purposes. However, the lack of acoustic logs or vertical seismic profiling in many older wells presents a significant challenge for accurate time-to-depth conversion, rendering this region relatively underexplored in this aspect, like many other mature basins around the world (Hart et al., 2000; Cao et al., 2017; Sun et al., 2023).

Traditionally, solving time-to-depth relationship (TDR) gaps within wells without acoustic logs or vertical seismic profiling relies on the implementation of velocity functions (hereafter referred to as extrapolation). These velocity functions contain information about the depth in the two-way travel time domain (hereafter referred to as TWT) derived from neighboring wells (Aker et al., 2020; Inichinbia and Saule, 2021; Al-Khazraji, 2023). Like any other assumption, this extrapolation could be erroneous which results in inaccuracies in time-to-depth conversion. This would influence every subsequent analysis and cause misinterpretation of the structures and lithofacies distribution in the subsurface which in turn is a crucial step in assessing hydrocarbon and/or geothermal reservoirs, as well as underground energy storage

Yandy Scientific Press

*Corresponding author.
E-mail address: akamenski@hgi-cgs.hr (A. Kamenski); marko.cvetkovic@rgn.unizg.hr (M. Cvetković); josipa.kapuralic@rgn.unizg.hr (J. Kapuralić); iva.kolenkovic@rgn.unizg.hr (I. Kolenković Močilac); ana.brckovic@rgn.unizg.hr (A. Brcković).

Received June 27, 2024; revised July 20, 2024; accepted August 12, 2024; available online August 17, 2024.

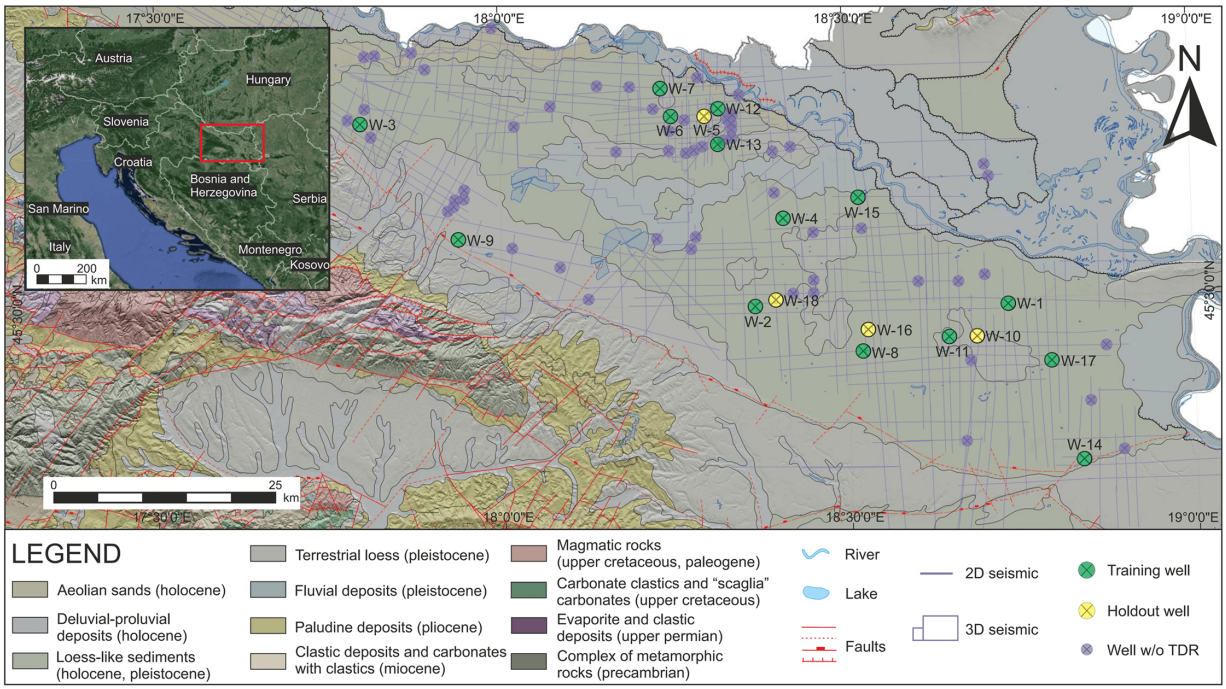

Fig. 1. Study area with well and seismic data displayed alongside basic surface geology adopted from the basic geological map of the Republic of Croatia 1:300,000 (HGI-CGS, 2009).

and CO_2 storage objects.

This research aims to investigate the feasibility of developing a more precise methodology for solving the TDR in cases with limited or no geophysical data. Initially, the accuracy of the conventional methodology was assessed in a way that TWT values were extrapolated from a nearby well. Subsequently, a methodology was developed for deriving TWT data for wells lacking acoustic logs or vertical seismic profiling, using artificial neural networks (ANNs) in combination with interpretation of basic well logs which were obtained even on older wells. Finally, results obtained using these two approaches were compared to show the average difference in the time-to-depth domain and the distribution of error from both methods.

The study aims to present a novel approach and assess its efficiency compared to traditional methods, potentially leading to significant cost savings in future subsurface explorations. Additionally, its application may unveil previously unknown correlations and dependencies within existing data, which would be beneficial for geo-energy exploration, not only in the Drava Basin but also in similar regions undergoing exploration.

2. Geological settings

Data prediction and analysis were performed on an area with a complex geological setting, situated in the eastern part of the Drava Basin which is in the southwestern part of the Pannonian Super Basin (Fig. 1).

Within the broader area of interest, three distinctive geological units can be distinguished. The first unit consists of the crystalline basement, primarily composed of partially metamorphosed Paleozoic magmatic rocks with the presence of metamorphosed sediments (Pamić and Lanphere, 1991; Pamić, 1998). The second unit is characterized by Mesozoic carbonates (Velić, 2007; Malvić and Cvetković, 2013), often referred to as "Base Tertiary" (Velić, 2007). The third unit includes Neogene and Quaternary sediments representing the basin infill (Saftić et al., 2003; Malvić and Cvetković, 2013).

The area experienced continental rifting from the Ottnangian to the Badenian periods, accompanied by a shift in stress orientation that led to sinistral transcurrent faults and the formation of narrow asymmetrical half-grabens (Lučić et al., 2001; Pavelić, 2001; Saftić et al., 2003; Pavelić and Kovačić, 2018). During the Otnnangian and Carpathian, sedimentation was predominantly characterized by coarse-grained clastic sediments deposited in alluvial to lacustrine environments. Meanwhile, sporadic occurrences of pyroclastics in the Drava Basin (Fig. 1) are related to the volcanic activity associated with rifting (Saftić et al., 2003).

A significant change in the depositional environment took place during Middle Badenian, due to marine transgression (Ćorić et al., 2009), which caused a shift from lacustrine to marine deposition. This transition resulted in sedimentation of thick marl layers with occurrences of coarse-grained clastic sediments, reflecting the occasional activity of gravity flows (Ćorić et al., 2009). Sarmatian is marked by the end of syn-rift extension and local compression (Saftić et al., 2003; Pavelić and Kovačić, 2018), as well as the isolation of Paratethys and accompanying salinity fluctuations (Pavelić and Kovačić, 2018). In these circumstances, deposition of coarse-grained clastic sediments, calcarenites, and limestones took place, whereas, in deeper parts of the basin, fine-grained sediments deposited, occasionally with sandstone occurrences resulting from sediment gravity flow (Pavelić and Kovačić, 2018).

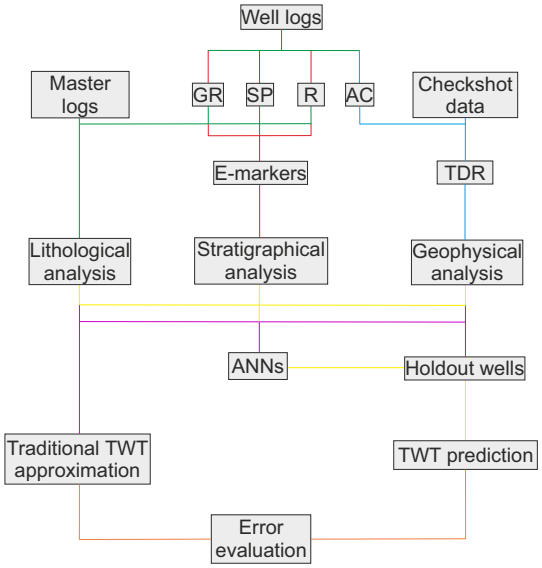

Fig. 2. Schematic representation of the workflow in which each line color represents the sequential process steps necessary for conducting each analysis from the provided input data.

During the Pannonian period, post-rift thermal subsidence took place (Lučić et al., 2001), due to the isostatic sinking of the crust thinned by mantle diapirism (Stegena et al., 1975), initially causing the deepening of the lake and deposition of deep-water marls (Pavelić and Kovačić, 2018). However, significant sediment supply without a corresponding increase in accommodation space resulted in the transition of sedimentation from lacustrine to deltaic environments, leading to the basin's infilling (Saftić et al., 2003; Pavelić and Kovačić, 2018). Neotectonics activity during the Pliocene and Quaternary resulted in compression and dextral transcurrent displacements, filling the remnants of Lake Pannon with coarse clastic sediments and clay. The Pleistocene glacial periods are marked by the deposition of loess sediments and aeolian sands (Wacha et al., 2013), while interglacial periods were marked by lacustrine and marsh sedimentation (Pavelić and Kovačić, 2018).

3. Data and methodology

This study aimed to develop a method for defining TDR that would be more reliable compared to extrapolation of the velocity functions from a neighboring well. This implies evaluating the data which has been almost always available within the well and which would have an impact on the change of velocities in the subsurface. All the historical well data had the basic Electrical well log curves which were employed to differentiate permeable and impermeable units and establish their boundaries, as well as to estimate fluid saturations. Units were correlated throughout the study area based on the interpretation of the resistivity and spontaneous potential curves, supplemented with other well data. These interpretations provided the basis for stratigraphic analysis. Another key part was to evaluate how many distinctive units with different lithological compositions could be defined in the studied area. This was evaluated from well reports based on the descriptions of lithology and selection of interpreted well markers.

This research utilized data from 18 wells (Fig. 1) drilled by the INA company as a part of their oil and gas exploration campaign between the 1980s and 2010s. The wells have an average depth of around 2,300 m, with Well-7 being the shallowest at 1,300 m depth and Well-3 being the deepest well with 4,110 m depth. These wells were selected based on the availability of acoustic well logs through the entire or the majority of the drilled section. The summarized workflow covering the entire process, from data preparation to the neural network deployment, is illustrated in Fig. 2.

Initially, a TDR was applied to all wells to enable transformation from measured depth to TWT domain for validation purposes. These steps are highlighted in blue in Fig. 2. The wells in which seismic velocity measurements or vertical seismic profiling data had been recorded were selected as input for the presented study (wells which are labeled in green and yellow in Fig. 1). The check-shot data were used to calibrate the acoustic logs with the check-shot travel times to create the TDRs for these 18 wells. Acoustic log calibration provides more accurate time-to-depth relationships and corrects for acoustic log drift due to equipment calibration issues, well conditions, or environmental factors (Mari et al., 2020). The calibration adjusts the acoustic log cumulative travel times to match the smoothed check-shot times. Prior to calibration, the acoustic logs were despiked. Despiking improves the overall quality of the acoustic logs by eliminating outliers and anomalies that do not represent the true properties of the subsurface (Rider, 2002).

Well logs, including gamma ray, spontaneous potential (SP), and short- and long-normal resistivity (R16, R64) were analyzed primarily to distinguish permeable and impermeable layers. Data preparation of these logs was performed in the Interactive Petrophysics software. Well logs are typically recorded in multiple intervals at various depths, necessitating the merging of these intervals. In our case, nearly every well log type required some form of conversion, rescaling, or normalization since well conditions change with every technical column due to the difference in temperature and mud properties (Bassiouni, 2013). Given the significance of the SP log and the common occurrence of SP inversion in certain sections of the log, the initial step involved analyzing the resistivity and gamma ray logs to identify inversed SP intervals. The occurrence of inversed intervals is due to the extremely low mineralization of the formation water, which can be below 5 g/l at several thousand meters of depth in the Drava Basin (Pavlin, 2022). Once these intervals were determined, they were assigned appropriate SP values for shale and clean formation, to ensure their reliability in further analyses.

Creation of TDRs, as well as lithological and stratigraphic interpretation were conducted in the Schlumberger Petrel software. This was followed by the differentiation of permeable from impermeable intervals per meter resolution. Regional well log markers were identified on the resistivity curve, defining boundaries of stratigraphic units (1-4). This characterization provided input parameters for ANN analysis.

ANNs are computational models inspired by the archi-

tecture and functionality of biological neural networks in the human brain. They comprise interconnected nodes, or "neurons", that process and transmit data (Prieto et al. (2016) and references therein).

The input parameters for the ANNs learning process consisted of three variables. Firstly, the true vertical depth subsea and the ratio of cumulative "sandstone to shale" ratio (S_s/S_h) both serve as continuous input variables. Here, S_s denotes the cumulative thickness of permeable layers up to a certain depth, while S_h represents the cumulative thickness of impermeable layers as one of the controlling factors of the velocity distribution in the subsurface. The third input variable denotes the categorical variable type, namely the stratigraphic category of the unit situated at the observed depth/case. These categories represent assigned values ranging from 1 to 4 which were defined by the stratigraphic differentiation conducted using interpreted well log markers. Finally, these input parameters were the basis for the ANNs prediction of TWT.

The analysis was conducted in TIBCO Statistica software using a regression approach for the time series. Networks were configured as multi-layer perceptron (MLP). MLPs are a type of artificial neural network with multiple layers of nodes, which process and transmit information (Thimm and Fiesler, 1997). Out of 18 wells, 14 were utilized for training the neural networks, while four were reserved for testing ANN on holdout data (Fig. 1). Neural network architecture was restricted to a minimum of three and a maximum of 17 neurons in the hidden layer. To mitigate overfitting during neural network training, a smaller value of weight decay was applied to enhance the network training. Weight decay penalizes large weights, thereby promoting the development of a simpler and more generalized model structure and ultimately enhancing performance on new, unseen data (Thimm and Fiesler, 1997).

Neural networks went through training, testing, and validation using a dedicated dataset consisting of four variables with a resolution of one meter. In total, there were more than 27,000 cases from 14 wells that were used for the training process of the neural networks. Ten neural networks with the most successful performance in training and testing were selected and used as an ensemble for the analysis (Hansen and Salamon, 1990). In a subsequent phase of ANNs analysis, trained neural networks were applied to predict target TWT values for four test wells (holdout wells) not included in the training process consisting of more than 8,000 cases.

The performance of the model was evaluated by calculating the error relative to the measured TWT values for each data point per resolution of one meter and calculating the absolute mean value for all cases within a well (orange steps in Fig. 2). For better visual comparison of the magnitude and distribution of the error, box and whiskers plots as well as maps illustrating error distribution were used.

4. Results

Well log interpretation, following the workflow shown in Fig. 2, enabled the differentiation of permeable and impermeable units. Moreover, the combination of these results with lithology data from Master logs enabled the definition of vertical lithology distribution which is displayed in the "Lithology" column in Fig. 3. Additionally, a maximum of four stratigraphic intervals were interpreted for each well. These intervals represent sediments of an age interval, similar in lithology and, if applicable, sedimentary environment as factors that can influence the change of petrophysical properties of rocks with burial. The first interval represents Pliocene-Quaternary unconsolidated sands, clays, gravels, and occasional coals. The second interval consists of Upper Miocene-Pannonian, which are predominantly sandstones and marls. The third interval represents a lithologically heterogeneous sediment of Lower and Middle Miocene breccias, conglomerates, sandstones, marls, and limestones, with sporadic occurrences of effusive. The fourth interval encompasses all rocks older than Miocene, including older pre-Neogene sediments as well as the metamorphic and magmatic complex comprising the Basement. One of the factors which was considered when the division was performed, was the impact of the present-day burial depth and its accompanying compaction and diagenetic processes influencing units' petrophysical properties. Consequently, it was presumed that the largest change of interval velocities would be from Neogene infill to Basement Neogene rocks (from intervals three to four). This transition represents the change from the lithologies in which petrophysical properties are governed by compaction to lithologies where fractures play a crucial role in controlling petrophysical properties, including crystalline rocks or Triassic dolomites. Most of the selected wells have been drilled through the first three intervals and finished in the fourth as hydrocarbon accumulations at some locations were expected even in the Basement rocks.

The selection of a representative training dataset is paramount for successful ANNs prediction. As was already established, a comprehensive training dataset was defined, reflecting the complexities of geology and petrophysics in the subsurface. The dataset comprised 18 wells, partitioned into a training set of 14 wells and four holdout wells. Holdout wells were used to evaluate the ANN model on previously unseen data. Wells W-5, W-10, and W-16 were selected as holdout wells because they were comprised of all four stratigraphic intervals, while well W-18 was chosen to represent the case where only the first two stratigraphic intervals were developed. The holdout wells have significant geographical positions, being close to one or more training wells. This arrangement allowed for examining whether proximity is always the best criterion for selecting the source for data extrapolation.

Given the continuous nature of the input dataset, time series regression was selected to ensure sequence prediction, aligning with geological and geophysical principles. The neural network architecture was optimized using various parameters and validated through repeated training, testing, and validation processes. The resulting correlation coefficients per each ANN are presented in Table 1, encompassing training, test, and validation process phases.

The correlation coefficient of the training set exhibited an accuracy range between 0.995711 and 0.995877. The testing data displayed a high accuracy range of 0.997796 to 0.997986. Similarly, the validation dataset yielded comparable performance, with an accuracy range of 0.997811 to 0.997982.

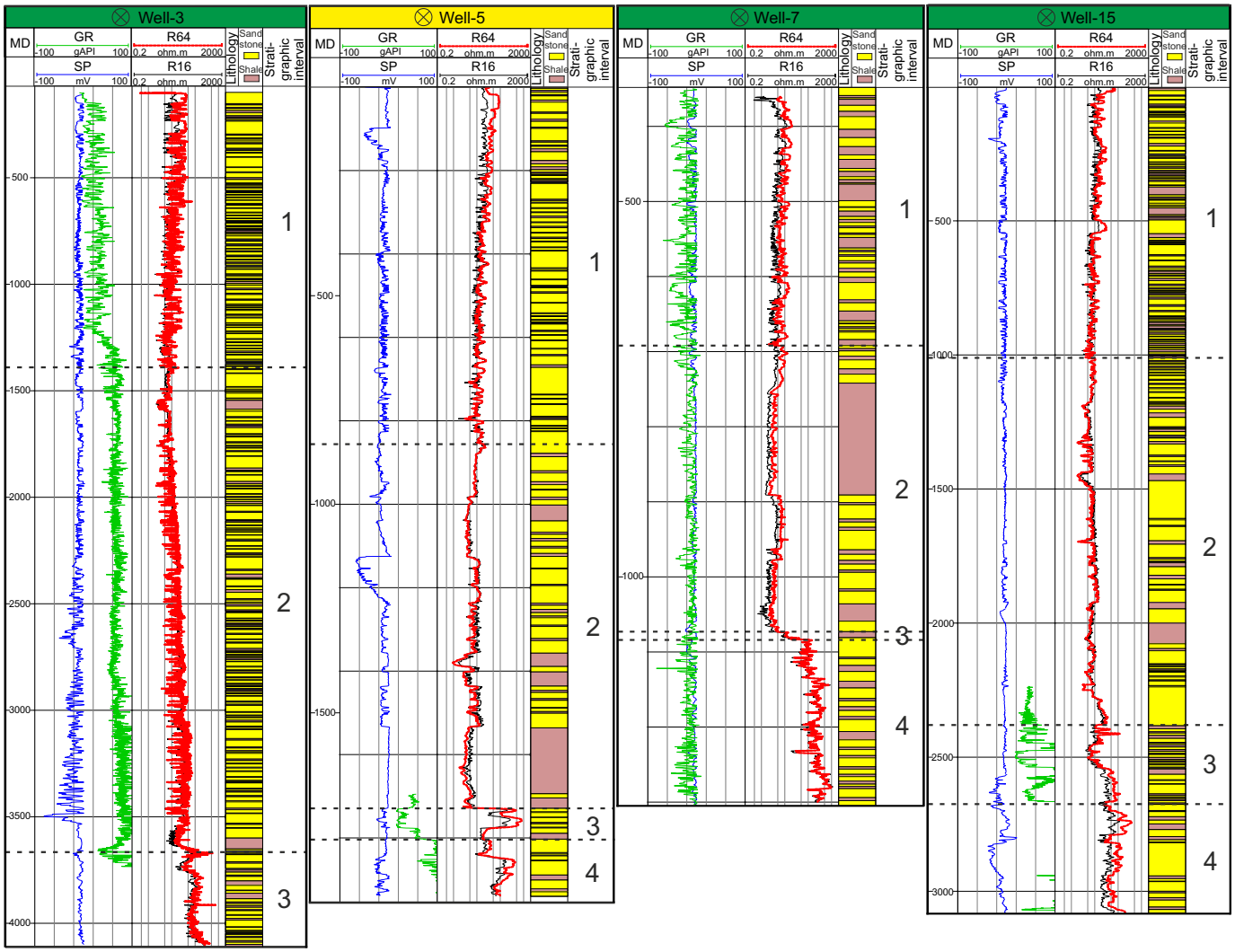

Fig. 3. Representation of the available well logs, interpretation of S_s and S_h as general lithology and stratigraphic intervals for four wells.

Table 1. Correlation coefficients, RMSE, MAE and RSQ of observed and predicted data for ten neural networks for training, test, and validation datasets from 14 wells.

Architecture	TWT train (ms)	TWT test (ms)	TWT validation (ms)	RMSE	MAE	RSQ
MLP 6-17-1	0.995770	0.997845	0.997878	34.008562	25.699704	0.995660
MLP 6-11-1	0.995823	0.997940	0.997967	33.426744	24.911437	0.995816
MLP 6-4-1	0.995716	0.997812	0.997829	34.364610	25.690295	0.995575
MLP 6-9-1	0.995831	0.997959	0.997937	33.399862	25.004618	0.995812
MLP 6-14-1	0.995852	0.997881	0.997911	33.568955	25.978290	0.995774
MLP 6-16-1	0.995877	0.997986	0.997982	33.111525	24.540709	0.995890
MLP 6-15-1	0.995743	0.997837	0.997848	34.237448	25.675535	0.995602
MLP 6-4-1	0.995845	0.997963	0.997971	33.256294	25.232209	0.995851
MLP 6-11-1	0.995804	0.997906	0.997895	33.734191	25.044579	0.995732
MLP 6-10-1	0.995711	0.997796	0.997811	34.499635	25.997086	0.995535

	W-1	W-2	W-3	W-4	W-5	W-6	W-7	W-8	W-9	W-10	W-11	W-12	W-13	W-14	W-15	W-16	W-17	W-18
W-1 Ev																		
W-2 Ev																		
W-3 Ev																		
W-4 Ev																		
W-5 Ev																		
W-6 Ev																		
W-7 Ev																		
W-8 Ev																		
W-9 Ev																		
W-10 Ev																		
W-11 Ev																		
W-12 Ev																		
W-13 Ev																		
W-14 Ev																		
W-15 Ev																		
W-16 Ev																		
W-17 Ev																		
W-18 Ev																		
Pv %	88,24%	58,82%	100,00%	88,24%	70,59%	82,35%	41,18%	76,47%	100,00%	88,24%	100,00%	100,00%	94,12%	100,00%	94,12%	82,35%	88,24%	82,35%

Fig. 4. A visual representation of the successfulness of the ANN prediction over the extrapolation approach. Well names used in the ANN training process are in green color, while holdout wells are highlighted in yellow. Cases with better Ev are labeled in red, while wells with better Pv are in green. Pv% represents a percentage of wells for which prediction via ANN gave more successful results while the green field indicates better results for Pv and the red field with the Ev approach.

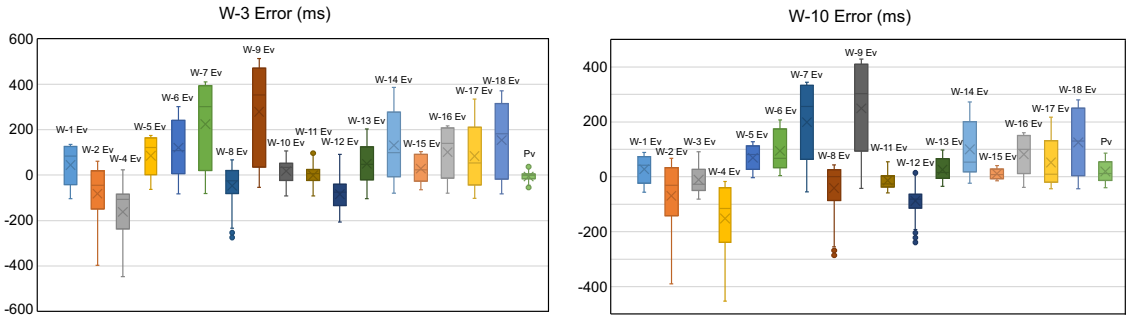

Fig. 5. Box and whisker plots representing the distribution of error in milliseconds (ms) for wells W-3 and W-10.

The root mean square error (RMSE) indicates that the average difference between values predicted by the ANN model and the actual values is approximately 34 ms. The mean absolute error (MAE) is even smaller, around 25 ms. The coefficient of determination (RSQ) value which is a measure of the goodness of the fit, demonstrates that the data fits the regression model very well. For prediction purposes, all ten neural networks were combined into an ensemble.

To evaluate the successfulness of the ANN deployment for the task, the TWT prediction results were compared to the TWT extrapolation values from nearby wells based on the average error relative to measured values from the well data. Error values were calculated for both the extrapolated TWT values versus measured values (Ev) and the ANN-predicted values versus measured TWT values (Pv). A matrix table was generated for each well to summarize these comparisons (Appendix 1).

When focusing solely on the success of the ANN prediction results, it is evident that 15 out of 18 wells show a closer fit to the measured values compared to those extrapolated from surrounding wells, i.e., they are more successful in over 75% of cases. It was found that for wells W-3, W-9, W-11, W-12, and W-14 prediction of TWT was outperforming the extrapolation method in 100% of cases (Fig. 4). Notably, four of these wells serve as holdout wells, indicated with yellow labels in Fig. 4 and Appendix 1. All of them achieved successful predicted values (Pv), with three demonstrating more than 80% more accurate outcomes than the extrapolation method (Fig. 4). Only a few instances showed smaller errors than those when TWT was predicted by the ANN analysis, highlighted in red in Appendix 1. The extrapolation approach achieved the best results for well W-7, with values from nine wells showing lower average errors.

Results are even better illustrated through the box and whisker plot (Fig. 5). The plot shows two representative wells: W-3, which was used in the ANN training process, and W-10, a holdout well. For W-3, ANN-predicted values exhibit the smallest average error compared to all errors calculated from extrapolating values from neighboring wells. In the case of W-10, there are only two instances (that correspond to extrapolations from W-11 and W-15) where the extrapolated values have a smaller error than the ANN-predicted values. Appendix 2 illustrates all case scenarios.

5. Discussion

The results of the ensemble ANN model demonstrate its ability to generate synthetic values for time-to-depth conversion using lithological parameters that can be interpreted from the most basic well logs and stratigraphic interval delineation. The trend observed in the predicted values closely aligns with

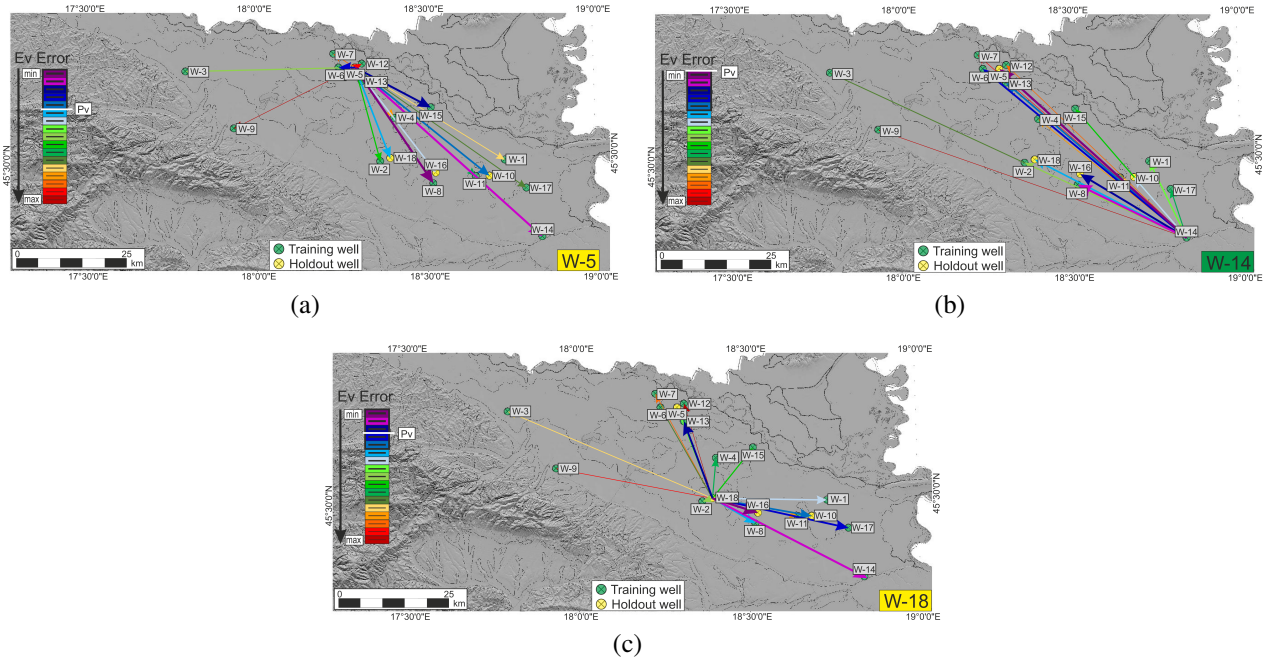

Fig. 6. Distribution of average errors obtained through extrapolation of TWT values from wells with available velocity information. The five best results, indicated by the smallest errors, are highlighted with thick arrows ranging in color from dark blue to dark purple (colors within the thick black rectangle in Ev Error Legend).

the measured values, as evidenced by the small average error, which ranges from a minimum of 11 ms to a maximum of 52 ms, with an average of 26 ms. Outlier and spread of the error are significantly lower when applying the ANN approach instead of an extrapolation of the TDR. Appendix 1 quantitatively presents the average errors, selected as the decisive parameter to evaluate the accuracy of ANN predictions.

The distribution of these errors and their relationship are illustrated in Fig. 6 for three representative cases and in Appendix 3 for all 18 cases. Upon thorough examination, several observations can be drawn. When extrapolating time-to-depth relationships, wells W-7, W-9 and W-12 consistently provide the largest errors (Appendix 2), indicating the poorest results for estimating TWT values in wells lacking velocity information. For Well-9, this is understandable given its greater distance from other wells in the area of exploration.

The analysis presents that proximity between wells does not guarantee accurate extrapolation of time-to-depth relations. Instead, the ANN predictions offer consistently more reliable results, even for the holdout wells which were never included in the building of the ANN model. This can be observed in Fig. 6 and Appendix 3. Despite the expectation that closely located wells would provide dependable time-to-depth information for extrapolation, the findings of this study disprove this assumption. For instance, in Fig. 6, case W-5 shows that wells W-7 and W-12, though remarkably close to well W-5 which is treated as a no velocity data well in this case scenario, yield extremely poor results with the highest errors compared to more distant wells.

This pattern is not uniform across all close pairs of wells. For example, extrapolating TWT values from W-6 to W-5 results in a satisfactory small average error of 21 ms. On the other hand, well W-2 despite being the closest, displays a poor correlation when extrapolating TWT information for W-18.

It is evident that, in most instances, extrapolating time-to-depth relations from nearby wells leads to significantly poorer outcomes compared to extrapolation from distant wells. This discrepancy could be attributed to substantial variations in subsurface lithology distribution and/or general orientation of structures.

The predicted values generated by the ANN analysis (indicated by the thick white line and “Pv” mark in the color legend in Fig. 5) demonstrate exceptional accuracy for both the training wells and, most importantly, the holdout wells (marked with green and yellow labels, respectively). With a high precision percentage observed, TWT values obtained through neural network analysis prove to be more reliable, especially for holdout wells (highlighted in yellow in Appendix 1, Fig. 6 and Appendix 3).

The distribution trend is also evident in Fig. 6, particularly highlighting the best five approximations. The results obtained from extrapolating TWT values reveal a predominant NNW-SSE strike, as observed in the top five approximations marked with the thickest arrows ranging from dark blue to dark purple. These findings are consistent with the strike of geological structures and sediment paleotransport orientation documented in recent investigations of the area (Rukavina et al., 2023; Špelić et al., 2023; Matošević et al., 2024).

6. Conclusion

Accurate determination of time-to-depth parameters plays a crucial role in various applications, including drilling opti-

mization and reservoir characterization. However, this process often entails significant economic and technical risks. To address these challenges and mitigate associated risks, a novel approach has been developed and is presented herein.

Building an ANN model to solve time-to-depth relationships has proven highly effective. The ANN model exhibits a high correlation coefficient for the training, testing, and validation set, all above 0.99, with root mean square errors under 35 ms and mean absolute errors around 25 ms. This level of accuracy surpasses any method applied so far on Pannonian Super Basin data, including the common approach of extrapolating values from nearby wells. The ANN model not only has smaller absolute errors but is also significantly less sensitive to outliers. Since model predictions depend on the local geological characteristics of the training data, a separate ANN model for solving TDRs should be developed for each basin or super-basin to account for their unique geological features.

Overall, this study presents the effectiveness of the ANN framework in conventional, dominantly clastic environments, tailored to the specific objectives of parameter prediction. Depending on the desired objective, the focus can vary from precise values to understanding broader trends and variations within the wells. This approach enhances efficiency and adaptability, improving the accuracy of subsurface models. The methodology remains open to further refinement through activities such as spatial information integration, hyper-parameter fine-tuning, and the development of tailored models for specific geological settings.

The results highlight the effectiveness of the proposed methodology in deriving TWT values from depth, lithological, and stratigraphical parameters by ANN analysis. This ANN-driven solution proves to be an effective approach for obtaining time-to-depth relations in mature basins with a large number of historical well data often lacking acoustic well log measurements and vertical seismic profiling.

Acknowledgements

This research was conducted as part of the research project founded by the Croatian Science Foundation (No. HRZZ UIP-2019-04-3846): “GEOlogical characterization of the Eastern part of the Drava depression subsurface intended for the evaluation of Energy Potentials (GEODEP)”. The authors would like to extend their gratitude to Schlumberger company for generously donating the Petrel academic software license. Additionally, we acknowledge the Croatian Hydrocarbon Agency for granting permission to access the data, without which the analysis presented in this paper would not have been possible.

Supplementary file

https://doi.org/10.46690/ager.2024.10.05

Conflict of interest

The authors declare no competing interest.

References

Aker, E., Tveiten, O. G., Wynn, T. Seismic pore pressure prediction at the Halten Terrace in the Norwegian Sea. Petroleum Geoscience, 2020, 26(2): 346-354.

Al-Khazraji, O. N. A. Cross-validation of time-depth conversion and evaluation of different approaches in the Mesopotamian Basin, Iraq. Exploration Geophysics, 2023, 54(3): 288-315.

Bassiouni, Z. Theory, Measurement, and Interpretation of Well Logs (4th edition). Texas, USA, Society of Petroleum Engineers, 2013.

Cao, J., Shi, Y., Wang, D., et al. Acoustic log prediction on the basis of kernel extreme learning machine for wells in GJH survey, Erdos Basin. Journal of Electrical and Computer Engineering, 2017, 2017: 3824086.

Ćorić, S., Pavelić, D., Rögl, F., et al. Revised Middle Miocene datum for initial marine flooding of North Croatian Basins (Pannonian Basin System, Central Paratethys). Geologia Croatica, 2009, 62(1): 31-43.

Hansen, L. K., Salamon, P. Neural network ensembles. IEEE Transactions on Pattern Analysis and Machine Intelligence, 1990, 12(10): 993-1001.

Hart, D. M., Balch, R. S., Weiss, W. W., et al. Time-to-depth conversion of nash draw “L” seismic horizon using seismic attributes and neural networks. Paper SPE 59555 Presented at SPE Permian Basin Oil and Gas Recovery Conference, Midland, Texas, 21-23 March, 2000.

HGI-CGS. Basic Geological Map of Croatia 1:300,000. Zagreb, Croatia, HGI-CGS, 2009.

Inichinbia, S., Saule, P. O. Well-to-seismic tie of a field onshore of the nigerian delta. Journal of Applied Sciences and Environmental Management, 2021, 25(1): 53-58.

Lučić, D., Saftić, B., Krizmanić, K., et al. The Neogene evolution and hydrocarbon potential of the Pannonian Basin in Croatia. Marine and Petroleum Geology, 2001, 18(1): 133-147.

Malvić, T., Cvetković, M. Lithostratigraphic units in the Drava Depression (Croatian and Hungarian parts)-a correlation. Nafta, 2013, 64(1): 27-33.

Mari, J. L., Vergniault, C., Coppens, F. Acoustic logging, in Well seismic surveying and acoustic logging, edited by J. L. Mari and C. Verginault, EDP Sciences, Paris, pp. 77-102, 2020.

Matošević, M., Garzanti, E., Šuica, S., et al. The Alps as the main source of sand for the Late Miocene Lake Pannon (Pannonian Basin, Croatia). Geologia Croatica, 2024, 77(2): 69-83.

Pamić, J. Crystalline basement of the South Pannonian Basin based on surface and subsurface data. Nafta, 1998, 49(12): 371-390.

Pamić, J., Lanphere, M. Hercynian granites and metamorphic rocks from the Mts. Papuk, Psunj, Krndija, and the surrounding basement of the Pannonian Basin in Slavonija (Northern Croatia, Yugoslavia). Geologija, 1991, 34(1): 81-253.

Pavelić, D. Tectonostratigraphic model for the North Croatian and North Bosnian sector of the Miocene Pannonian Basin System. Basin Research, 2001, 13(3): 359-376.

Pavelić, D., Kovačić, M. Sedimentology and stratigraphy of the Neogene rift-type North Croatian Basin (Pannonian Basin System, Croatia): A review. Marine and Petroleum Geology, 2018, 91: 455-469.

Pavlin, I. Formation water salinity in deep permeable layers in Eastern part of Drava Basin. Zagreb, University of Zagreb, 2022. (in Croatian)

Prieto, A., Prieto, B., Ortigosa, E. M., et al. Neural networks: An overview of early research, current frameworks and new challenges. Neurocomputing, 2016: 214: 242-268.

Rider, M. The Geological Interpretation of Well Logs (2nd edition). Sutherland, Scotland, Rider-French Consulting Ltd., 2002.

Rukavina, D., Saftić, B., Matoš, B., et al. Tectonostratigraphic analysis of the syn-rift infill in the Drava Basin, south-western Pannonian Basin System. Marine and Petroleum Geology, 2023, 152: 106235.

Saftić, B., Velić, J., Sztanó, O., et al. Tertiary subsurface facies, source rocks and hydrocarbon reservoirs in the SW part of the Pannonian Basin (Northern Croatia and south-western Hungary). Geologia Croatica, 2003, 56(1): 101-122.

Špelić, M., Kovács, Á., Saftić, B., et al. Competition of deltaic feeder systems reflected by slope progradation: A high-resolution example from the Late Miocene-Pliocene, Drava Basin, Croatia. International Journal of Earth Sciences, 2023, 112: 1023-1041.

Stegena, L., Géczy, B., Horváth, F. Late Cenozoic evolution of the Pannonian basin. Tectonophysics, 1975, 26(1-2): 71-90.

Sun, Z., Yang, S., Zhang, F., et al. A reconstructed method of acoustic logging data and its application in seismic lithological inversion for uranium reservoir. Remote Sensing, 2023, 15(5): 1260.

Thimm, G., Fiesler, E. High-order and multilayer perceptron initialization. IEEE Transactions Neural Networks, 1997, 8(2): 349-359.

Velić, J. Petroleum geology. Zagreb, University of Zagreb, 2007. (in Croatian)

Velić, J., Krasić, D., Kovačević, I. Exploitation, reserves and transport of natural gas in the Republic of Croatia. Tehnički Vjesnik-Technical Gazette, 2012a, 19(3): 633-641.

Velić, J., Malvić, T., Cvetković, M., et al. Reservoir geology, hydrocarbon reserves and production in the Croatian part of the Pannonian Basin System. Geologia Croatica, 2012b, 65(1), 91-101.

Wacha, L., Galović, L., Koloszár, L., et al. The chronology of the Šarengrad II loess-palaeosol section (Eastern Croatia). Geologia Croatica, 2013, 66(3): 191-203.